

# Terahertz reflectometry of burn wounds in a rat model

M. Hassan Arbab,<sup>1,2,\*</sup> Trevor C. Dickey,<sup>1,3</sup> Dale P. Winebrenner,<sup>1,2</sup> Antao Chen,<sup>1,2</sup>  
Mathew B. Klein,<sup>4</sup> and Pierre D. Mourad<sup>1,3,5</sup>

<sup>1</sup>Applied Physics Laboratory, University of Washington, 1013 NE 40th Street, Seattle, Washington 98105-6698, USA

<sup>2</sup>Department of Electrical Engineering, University of Washington, 185 Stevens Way,  
Paul Allen Center, Seattle, Washington 98195-2500, USA

<sup>3</sup>Department of Neurological Surgery, University of Washington,  
1959 NE Pacific Street, Seattle, Washington 98195-6470, USA

<sup>4</sup>Burn Center and Division of Plastic Surgery, Department of Surgery, University of Washington,  
325 9th Avenue, Seattle, Washington 98104, USA

<sup>5</sup>Department of Bioengineering, University of Washington,  
3720 15th Avenue NE, Seattle, Washington 98195-5061, USA

\*mharbab@uw.edu

**Abstract:** We present sub-millimeter wave reflectometry of an experimental rat skin burn model obtained by the Terahertz Time-Domain Spectroscopy (THz-TDS) technique. Full thickness burns, as confirmed by histology, were created on rats ( $n = 4$ ) euthanized immediately prior to the experiments. Statistical analysis shows that the burned tissue exhibits higher reflectivity compared to normal skin over a frequency range between 0.5 and 0.7 THz ( $p < 0.05$ ), likely due to post-burn formation of interstitial edema. Furthermore, we demonstrate that a double Debye dielectric relaxation model can be used to explain the terahertz response of both normal and less severely burned rat skin. Finally, our data suggest that the degree of conformation between the experimental burn measurements and the model for normal skin can potentially be used to infer the extent of burn severity.

©2011 Optical Society of America

**OCIS codes:** (300.6495) Spectroscopy, terahertz; (170.4580) Optical diagnostics for medicine; (170.6795) Terahertz imaging; (170.6510) Spectroscopy, tissue diagnostics; (170.1610) Clinical applications.

---

## References and links

1. R. Gómez and L. C. Cancio, "Management of burn wounds in the emergency department," *Emerg. Med. Clin. North Am.* **25**(1), 135–146 (2007).
2. B. S. Atiyeh, S. W. Gunn, and S. N. Hayek, "State of the art in burn treatment," *World J. Surg.* **29**(2), 131–148 (2005).
3. J. M. Still, E. J. Law, K. G. Klavuhn, T. C. Island, and J. Z. Holtz, "Diagnosis of burn depth using laser-induced indocyanine green fluorescence: a preliminary clinical trial," *Burns* **27**(4), 364–371 (2001).
4. M. A. Afromowitz, J. B. Callis, D. M. Heimbach, L. A. DeSoto, and M. K. Norton, "Multispectral imaging of burn wounds: a new clinical instrument for evaluating burn depth," *IEEE Trans. Biomed. Eng.* **35**(10), 842–850 (1988).
5. H. A. Green, D. Bua, R. R. Anderson, and N. S. Nishioka, "Burn depth estimation using indocyanine green fluorescence," *Arch. Dermatol.* **128**(1), 43–49 (1992).
6. M. J. Koruda, A. Zimble, R. G. Settle, D. O. Jacobs, R. H. Rolandelli, G. L. Wolf, and J. L. Rombeau, "Assessing burn wound depth using in vitro nuclear magnetic resonance (NMR)," *J. Surg. Res.* **40**(5), 475–481 (1986).
7. A. D. Jaskille, J. C. Ramella-Roman, J. W. Shupp, M. H. Jordan, and J. C. Jeng, "Critical review of burn depth assessment techniques: part II. Review of laser doppler technology," *J. Burn Care Res.* **31**(1), 151–157 (2010).
8. S. Iraniha, M. E. Cinat, V. M. VanderKam, A. Boyko, D. Lee, J. Jones, and B. M. Achauer, "Determination of burn depth with noncontact ultrasonography," *J. Burn Care Rehabil.* **21**(4), 333–338 (2000).
9. A. Papp, T. Lahtinen, M. Härmä, J. Nuutinen, A. Uusaro, and E. Alhava, "Dielectric measurement in experimental burns: a new tool for burn depth determination?" *Plast. Reconstr. Surg.* **117**(3), 889–898 (2006).

10. S. M. Srinivas, J. F. de Boer, H. Park, K. Keikhanzadeh, H. E. Huang, J. Zhang, W. Q. Jung, Z. Chen, and J. S. Nelson, "Determination of burn depth by polarization-sensitive optical coherence tomography," *J. Biomed. Opt.* **9**(1), 207–212 (2004).
11. M. G. Sowa, L. Leonardi, J. R. Payette, K. M. Cross, M. Gomez, and J. S. Fish, "Classification of burn injuries using near-infrared spectroscopy," *J. Biomed. Opt.* **11**(5), 054002 (2006).
12. K. M. Cross, L. Leonardi, J. R. Payette, M. Gomez, M. A. Levasseur, B. J. Schattka, M. G. Sowa, and J. S. Fish, "Clinical utilization of near-infrared spectroscopy devices for burn depth assessment," *Wound Repair Regen.* **15**(3), 332–340 (2007).
13. P. H. Siegel, "Terahertz technology in biology and medicine," *IEEE Trans. Microw. Theory Tech.* **52**(10), 2438–2447 (2004).
14. E. Pickwell and V. P. Wallace, "Biomedical applications of terahertz technology," *J. Phys. D Appl. Phys.* **39**(17), R301–R310 (2006).
15. A. J. Fitzgerald, E. Berry, N. N. Zinov'ev, S. Homer-Vanniasinkam, R. E. Miles, J. M. Chamberlain, and M. A. Smith, "Catalogue of human tissue optical properties at terahertz frequencies," *J. Biol. Phys.* **29**(2/3), 123–128 (2003).
16. E. Pickwell, B. E. Cole, A. J. Fitzgerald, V. P. Wallace, and M. Pepper, "Simulation of terahertz pulse propagation in biological systems," *Appl. Phys. Lett.* **84**(12), 2190–2192 (2004).
17. E. Pickwell, B. E. Cole, A. J. Fitzgerald, M. Pepper, and V. P. Wallace, "In vivo study of human skin using pulsed terahertz radiation," *Phys. Med. Biol.* **49**(9), 1595–1607 (2004).
18. D. M. Mittleman, M. Gupta, R. Neelamani, R. G. Baraniuk, J. V. Rudd, and M. Koch, "Recent advances in terahertz imaging," *Appl. Phys. B* **68**(6), 1085–1094 (1999).
19. Z. D. Taylor, R. S. Singh, M. O. Culjat, J. Y. Suen, W. S. Grundfest, H. Lee, and E. R. Brown, "Reflective terahertz imaging of porcine skin burns," *Opt. Lett.* **33**(11), 1258–1260 (2008).
20. Q. Wu and X.-C. Zhang, "Free-space electro-optic sampling of terahertz beams," *Appl. Phys. Lett.* **67**(24), 3523–3525 (1995).
21. P. U. Jepsen, D. G. Cooke, and M. Koch, "Terahertz spectroscopy and imaging – modern techniques and applications," *Laser Photon. Rev.* **5**(1), 124–166 (2011).
22. R. M. Woodward, B. E. Cole, V. P. Wallace, R. J. Pye, D. D. Arnone, E. H. Linfield, and M. Pepper, "Terahertz pulse imaging in reflection geometry of human skin cancer and skin tissue," *Phys. Med. Biol.* **47**(21), 3853–3863 (2002).
23. J. T. Kindt and C. A. Schmuttenmaer, "Far-infrared dielectric properties of polar liquids probed by femtosecond terahertz pulse spectroscopy," *J. Phys. Chem.* **100**(24), 10373–10379 (1996).
24. T. W. Panke and C. G. McLeod, *Pathology of Thermal Injury: a Practical Approach* (Grune & Stratton, 1985).
25. A. M. I. Watts, M. P. H. Tyler, M. E. Perry, A. H. N. Roberts, and D. A. McGrouther, "Burn depth and its histological measurement," *Burns* **27**(2), 154–160 (2001).

## 1. Introduction

### 1.1 Assessment of Burn Injuries

Each year over one million burn injuries receive medical attention in the United States, resulting in about 45,000 hospitalizations [1]. Traditionally, burn wounds are stratified based on the depth of injured skin into three clinically useful categories [2]. The depth of a first degree, or superficial burn, is limited to the epidermal layer of the skin and these injuries heal spontaneously. Second degree or partial thickness burns involve the entire epidermis and a portion of the dermis. The depth of dermal injury can vary within this group, with wounds of greater depth requiring longer time to heal. A third degree burn injures the full thickness of the skin - the epidermis and the entirety of the dermis - and typically requires surgical excision and skin grafting. Management of burn injuries requires determination of the layers of skin that are damaged, as this will guide treatment either towards wound care with ultimate spontaneous healing or surgical treatment. The accuracy rate of clinical assessments by experienced physicians, is only about 64-70% for partial-thickness burns [3]. This rate is even lower (50-65%) for differentiating the subgroup of burn wounds that will not heal without surgical procedures [2].

This problem has motivated research on the development of a wide variety of methods and technologies to aid the clinical assessment of burns, including multispectral optical reflection imaging [4], Indocyanine green dye fluorescence techniques [3,5], Nuclear Magnetic Resonance (NMR) imaging [6], Laser Doppler Imaging (LDI) [7], ultrasonography [8], contact dielectric measurement at radio frequencies [9], Polarization-Sensitive Optical Coherence Tomography (PS-OCT) [10], and near infrared spectroscopy [11,12]. However,

widespread adoption of the aforementioned techniques in routine patient care is significantly hindered by practical concerns for accuracy, cost effectiveness, and compatibility in clinical environments [2].

### 1.2 Biomedical Applications of Terahertz Technology

Biological and biomedical applications of terahertz technology have attracted much attention in the recent years [13]. The high sensitivity of terahertz radiation to absorption by both bound and free water molecules gives rise to many of these applications [14]. Moreover, due to their low photon energies (1–12 meV), terahertz emissions are non-ionizing and therefore safe for cellular level investigations [13]. Fitzgerald *et al.* showed that distinct human tissues differ in their optical properties at terahertz frequencies, including e.g., striated muscle, adipose tissue, and skin [15]. Pickwell and colleagues showed that the terahertz reflection response of healthy human skin follows a double Debye model, which is predominantly determined by the effective water content of different skin layers [16,17]. The first application of terahertz technology for imaging burns was to severely burned chicken muscle tissue [18]. Taylor *et al.* used radiation at a center frequency of 0.5 THz with 125 GHz bandwidth to image thermal damage induced by branding previously-frozen porcine skin grafts at 315°C for 3 seconds [19]. They concluded that removal of water from the burned sections of the excised skin samples resulted in lower terahertz reflectivity compared to the healthy parts of the skin.

In this paper, we present terahertz reflectometry results from an experimental animal model that includes fresh full-thickness skin and underlying tissue, in contrast to the previously cited papers. Here, the observed formation of post-burn interstitial edema likely caused the observed increase in terahertz reflectivity of the burns. Furthermore, our analysis shows that the double Debye dielectric relaxation model proposed by Pickwell *et al.* [16] can be extended to successfully explain the terahertz response of less severe burn samples. Finally, we used an image processing approach, for the analysis of the histological information from the burned tissues, to establish a quantifiable measure of the burn severity based on a reduction in the number and size of the intact skin structures. Our analysis suggests that as the severity of the burn increases, the agreement between the terahertz spectral response and the theoretical model for normal skin decreases. This technique can potentially be used to assess the severity of the burns according to the degree of conformation of terahertz measurements with the model presented.

## 2. Experimental Methods

### 2.1 Animal Model and Burn Protocol

The experimental protocol used in this study was approved by the Institutional Animal Care and Use Committee at the University of Washington, Seattle. Male Sprague-Dawley rats ( $n = 4$ ), weighing between 360 and 600 g, were anesthetized with isoflurane (4% for induction, 2% for maintenance, each with O<sub>2</sub> flow rate of 1 liter/minute). After the animal was anesthetized, its back was shaved and epilated with hair remover lotion (Nair, Church & Dwight Co, Princeton, NJ). Two posterior sites corresponding to approximately the 12th thoracic vertebra, as verified later via autopsy, were marked 3 cm laterally off from the midline on either sides of the rats. One of these two sites was used to create a burn and the other site was reserved as a source of control tissue. We followed a burn induction protocol similar to those discussed in the literature [5,6,10]. Specifically, a 313 g brass rod, with a 1 cm diameter cylindrical protrusion, was heated in a water bath maintained at 100°C. The rats were euthanized using an overdose of pentobarbital (250 mg/kg) within 5 minutes prior to the application of the brass rod to the skin. The cylindrical protrusion was then held against the marked site for 30 seconds using only the weight of the rod. After the terahertz experiments, biopsy samples were collected using a 3 mm biopsy punch. Histological analysis of the H&E-stained samples

confirmed a full-thickness 3rd degree burn. Figure 1(a)–1(c) shows one such burn along with a representative histological section microscope image of both burned and control normal tissue. Formation of interstitial edema, as expected from the biological response of tissue to thermal burns [2], is visible in Fig. 1(a). Also, in Fig. 1(b) and 1(c), a reduction in number and volume of discrete skin structures, which are comparable in size to the wavelength of the THz radiation, can be observed in burned compared to normal skin.

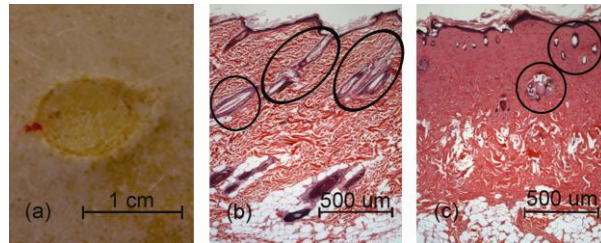


Fig. 1. (a) Image of a 100°C, 30 second burn, along with a sample histological cross section of (b) normal and (c) burned skin confirms the existence of a 3rd degree burn. Note that post-burn edema is evident in (a) as well as the reduction in the number and size of discrete normal skin structures (marked) in burned skin relative to normal skin.

## 2.2 Terahertz Spectroscopy Technique

The Terahertz Time-Domain Spectroscopy (THz-TDS) setup used for obtaining reflections from normal and burned skin has been explained in the literature [20,21]. Briefly, a photoconductive antenna with 100  $\mu\text{m}$  gap, built on low-temperature grown GaAs, generated terahertz waves, which were then focused using a pair of off-axis parabolic mirrors through a 1.588 mm thick fused silica plate on the skin and detected via the electro-optic sampling method in a ZnTe crystal. The entire THz-TDS system was enclosed in a box and purged with dry  $\text{N}_2$  gas throughout the experiments. Using an imaging window has many advantages, including flattening the surface of the skin at the point of measurement and allowing for higher reflectivity at the window/skin interface [17]. However, it also gives rise to the presence of a baseline terahertz waveform, which is reflected from the first air/window boundary and is superimposed with the desired time-domain signal from the second interface with the skin. In order to remove the effect of the baseline interference, we used reference reflection measurements from an 3.175 mm thick fused silica slab, similar to the method explained by Woodward *et al.* [22]. The reflection from this thicker slab was then aligned with and subtracted from the terahertz signal reflected from the thinner window and air boundary, in the time-domain, to give a “Differential Reference.” Similarly, the thicker window reference was aligned with and subtracted from all subsequent normal and burned skin measurements.

Skin tissue is an inhomogeneous medium, consisting of hair follicles, sweat glands, etc, which are comparable in size to the radiation wavelength. To compensate for this source of tissue variability, for each skin sample the average of several (3–5) spatially disjoint terahertz measurements was calculated. The spot size of the terahertz beam was approximately 2 mm at the focal point. Figure 2 shows the Differential Reference and the terahertz reflection measurements from the normal and burned skin of one of the rat samples. Before employing the Fast Fourier Transform (FFT) to investigate the spectral dependence of normal and burned skin samples, a split cosine taper was multiplied by the first and last 20 to 25 points of the time series and additional zeros were padded to both ends. The FFT amplitudes of the samples were normalized by the FFT of the Differential Reference to eliminate the effect of the intrinsic system response function. Moreover, to account for a typical terahertz signal amplitude drift in between measurements, the signal peak from the first interface of the slab,

between air and fused silica, was used to self-calibrate each measurement with that of the references. As shown in the inset of Fig. 2, for the frequency range between 0.4 and 0.7 THz, the magnitude of the reflected Spectral Amplitude (S.A.) from this example of burned skin is significantly larger than reflection from the normal tissue.

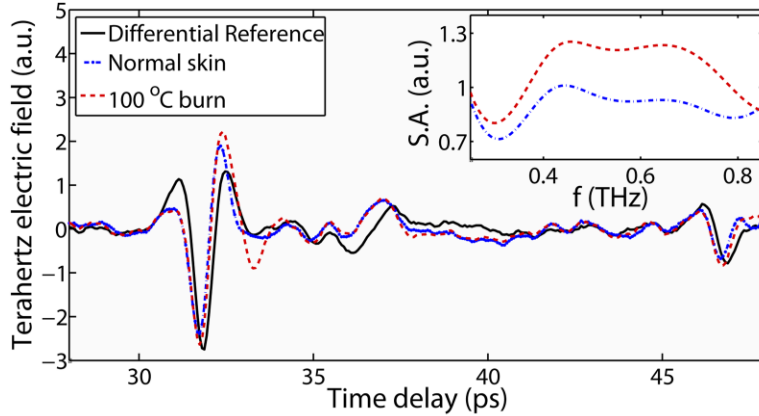


Fig. 2. Representative terahertz time-domain reflection measurement from normal and burned skin after removal of the baseline interference waveform, along with the Differential Reference. Inset: normalized FFT Spectral Amplitudes (S.A.) of the same time-domain signals.

### 3. Results and Discussion

Figure 3(a) summarizes the contrast between normal and burned skin samples for all of our measurements at four chosen frequency points between 0.4 and 0.7 THz, along with the standard deviation error bars. The results indicate a statistically significant ( $p < 0.05$ ) contrast over the 0.5–0.7 THz range. We also used Eq. (1), below, to calculate a measure of the normalized excess reflectivity from the skin burns compared to the normal tissue,

$$\frac{r_b - r_n}{r_n} \times 100, \quad (1)$$

where  $r_b$  and  $r_n$  are the Fourier reflection amplitudes of the burned and normal skin, respectively. Figure 3(b) shows this quantity in a whisker plot, where the boxes contain the 5% to 95% of the data range (with the remaining values in the whiskers) and the mean line indicated at each frequency point. It is evident that, on average,  $r_b > r_n$  by at least about 30%. Our results contrast with those of Taylor *et al.* [19] in excised porcine skin burns, which can be attributed to the large difference in the temperatures used for burn induction in these two studies, as well as the formation of interstitial edema in our animal model (see Fig. 1(a)), which cannot be observed in skin grafts samples. This excess intercellular liquid results in higher effective water content in the burned tissue [9], which in turn determines the terahertz reflection response of the skin layers [16,17]. It should also be noted that the local production of excess liquid here is likely due to cellular breakdown and is therefore etiologically different from the vascular edema that can be expected in live models.

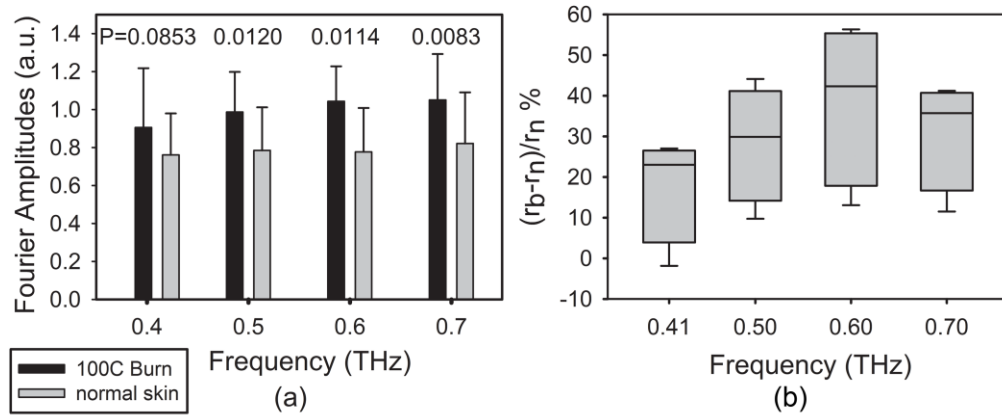


Fig. 3. (a) Histogram of the average and standard deviation of the reflection spectral amplitudes from normal and burned skin at four frequency points. The observed contrast is statistically significant ( $p < 0.05$ ) at 0.5, 0.6, and 0.7 THz. (b) The whisker plot represents the normalized difference between terahertz reflectivity of burned and normal skin.

### 3.1 Double Debye Dielectric Model

To better understand the change in the dielectric properties of skin post burn injuries, we employed the double Debye dielectric relaxation model, as presented in Eq. (2),

$$\hat{\epsilon}(\omega) = \epsilon_{\infty} + \frac{\epsilon_s - \epsilon_2}{1 + i\omega\tau_1} + \frac{\epsilon_2 - \epsilon_{\infty}}{1 + i\omega\tau_2}, \quad (2)$$

where  $\epsilon_s$  and  $\epsilon_{\infty}$  are respectively the static and high frequency limiting dielectric constants, and  $\epsilon_2$  is an intermediate dielectric value.  $\tau_1$  and  $\tau_2$  are time constants associated with a combination of different relaxation processes of hydrogen bonds and structural rearrangements. The utility of this model to predict the terahertz response of various polar liquids have been shown previously [23]. Pickwell *et al.* successfully coupled this model with a Finite-difference Time-domain (FDTD) representation of the Maxwell's equations to simulate the propagation of terahertz waves in healthy human skin samples [16,17]. Table 1 summarizes the published values for the double Debye constants of water and healthy human skin, extracted from similar THz-TDS measurements. Table 1 also lists the range of  $\tau_1$  values that were obtained by performing a least square fit to our terahertz reflection measurements from each of the euthanized rat skin samples.

**Table 1. Double Debye Parameters for Water, Healthy Human and Rat Skin**

	$\epsilon_{\infty}$	$\epsilon_2$	$\epsilon_s$	$\tau_1$ (ps)	$\tau_2$ (ps)
Water (transmission) <sup>a</sup>	3.5	4.9	78.4	8.2	0.18
Water (reflection) <sup>b</sup>	4.1	6.6	78.8	10.6	0.18
Human skin (volar forearm) <sup>b</sup>	3.0	3.6	60.0	10.0	0.20
Human skin (epidermis) <sup>c</sup>	3.0	3.6	58	9.4	0.18
Euthanized rat normal skin (dorsal)	3.0	3.6	60.0	<2.2 – 5.19>	0.2

<sup>a</sup> From Kindt and Schmittenmaer *J. Phys. Chem.* **100**, 10373 (1996).  
<sup>b</sup> From Pickwell *et al. APL* **84**, 2190 (2004).  
<sup>c</sup> From Pickwell *et al. Phys. Med. Biol.* **49**, 1595 (2004).

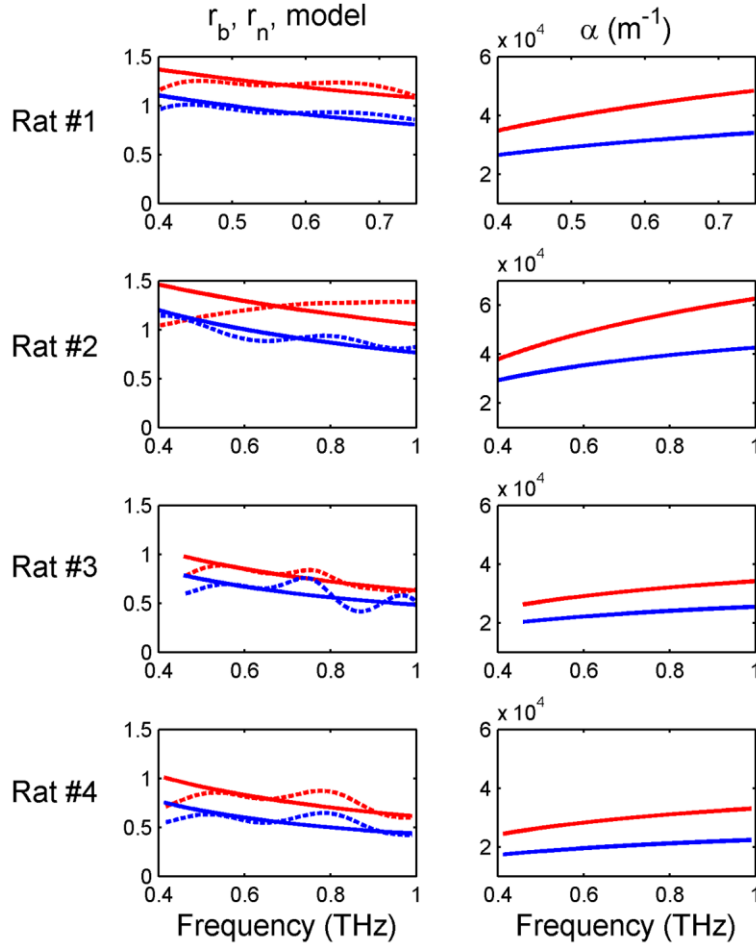


Fig. 4. Left column panels plot the Fourier amplitudes of the experimental terahertz reflectivity of normal (dotted blue lines) and burned tissue (dotted red lines). The solid lines show the double Debye model fits. Right column shows the calculated absorption coefficient for each burned and normal sample from the model parameters.

We note that a small degree of variation was previously reported in the terahertz response of healthy human skin, from the same volunteer, over the course of 4 weeks [17], which is presumably due to change in the hydration level of skin. Figure 4 shows the results of this analysis on both normal skin samples (control experiment) as well as the burns on each rat in our study. It should be pointed out that in this analysis, all double Debye parameters have been kept constant and set to the human skin values as given by Ref. 16 except for  $\tau_1$ . As the fit in the burn measurements indicates, the degree to which the experimental results and the model conform varies among our skin tissue samples. We defined the normalized error of the least square optimization by

$$error = \sum_f \frac{(|r_{\text{exp}}| - |r_{\text{model}}|)^2}{\sigma^2}, \quad (3)$$

where  $r_{\text{exp}}$  is the Fourier amplitudes of normalized measured reflected terahertz electric field and  $\sigma^2$  is the variance of the measurement.



While all rats were subjected to the same burn protocol, as anticipated from the variation in the thickness of the skin layers and the fluctuations in the biological constituents of the tissue, the severity of the final burns were different. This phenomenon can be noted in the histological cross section images of both normal and burned skin in Fig. 5. In order to quantify this subtle source of sample variation, an image processing routine was used to identify and calculate the density of the discrete structures in the histological images. The algorithm first identifies the skin edge and subsequently defines a search area approximately 400  $\mu\text{m}$  deep in the tissue. It then recognizes tissue structures such as microvascular blood capillaries, hair follicles, sweat glands, and their skin tunnels, etc. based on the ratio of the red and blue components of the acquired image. Finally, the program calculates the total areal density of such structures within the search area. Figure 5 shows typical outcomes of the image processing routine for both normal and burn samples. (Histological information for rat #1 was not available.)

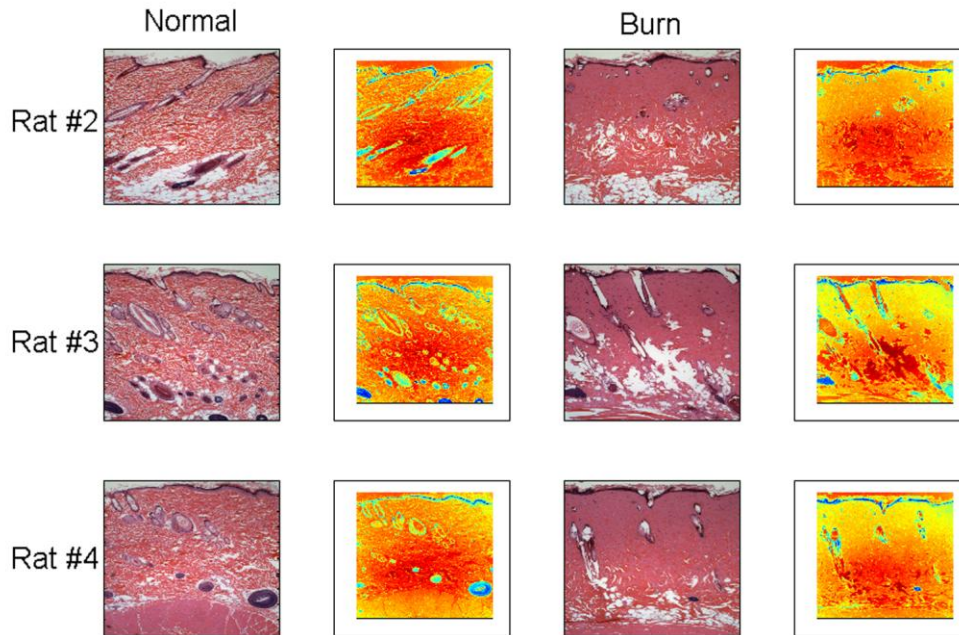


Fig. 5. Histological section images of normal (control experiment) and 100°C, 30 second burn injuries are shown along with their respective outputs of the image processing routine.

Figure 6 shows that as the density of discrete intact structures in the skin decreases (as a result of burn injury), the degree of conformation between the double Debye model and the experimental results, as calculated by Eq. (3), decreases. These preliminary results suggest that the terahertz response of skin burns is not only a function of the biological content in the tissue, most notably water, but also it is sensitive to the number and size of the intact skin structures. These structures, which are known to be determinants of the healing likelihood of the burned skin [10,11,24,25], can give rise to scattering of electromagnetic waves as they propagate through skin layers. Therefore, it can be inferred that the amount of deviation of the terahertz measurements from the double Debye model for normal skin can potentially be used as an indicator for the degree to which the tissue is injured.



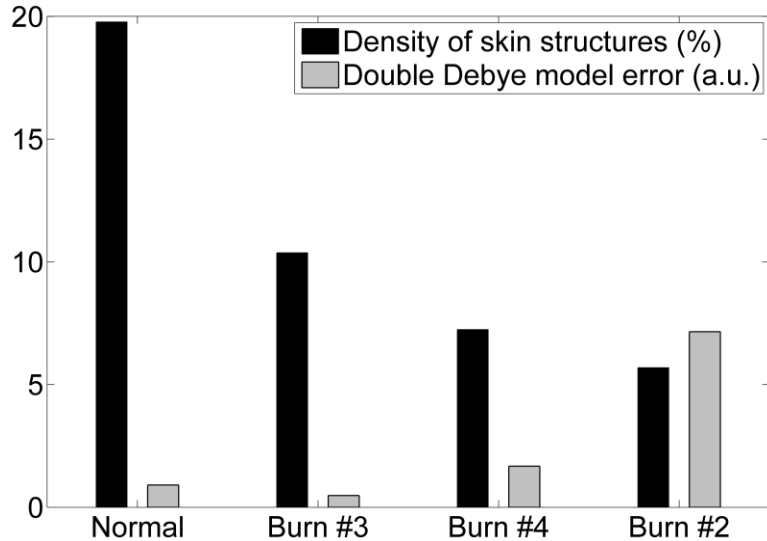


Fig. 6. Comparison between the severity of the burn injuries, as indicated by the density of intact skin structures, and the degree of conformation of the experimental results to the double Debye model. The vertical axis is dimensionless (see text).

#### 4. Conclusion

We have presented terahertz reflectometry results obtained from acutely burned and normal skin of a rat model. The results show that the terahertz reflectivity of a 3rd degree burn is higher than that of normal skin by about 30% in a frequency range between 0.5 and 0.7 THz ( $p < 0.05$ ). This contrast is likely due to the post-burn formation of interstitial edema which results in higher water content in the burned sites. We have shown that the empirical double Debye dielectric relaxation model can be extended, by optimizing only one parameter, to conform to the experimental results from both normal rat skin and less severe burn injuries. Furthermore, our preliminary analysis of the burn severity, given by the density of intact skin structures in post-burn histology, suggests that the sensitivity of terahertz radiation to a reduction in the number and size of these structures can be exploited to assay burn grades. Future work on in-vivo experimental reflectometry of various burn grades, involving both acute and survival studies, is necessary to further advance the potential clinical application of terahertz spectroscopy in burn diagnosis.

#### Acknowledgments

MHA would like to thank Dr. Eric I. Thorsos for valuable discussions and for reviewing the first draft of the manuscript. This work was partially sponsored by the Washington Research Foundation (WRF Capital).